Neyman–Pearson Criterion-Based Change Detection Methods for Wavelength–Resolution SAR Image Stacks

Dimas I. Alves, Crístian Müller, Bruna G. Palm, Mats I. Pettersson, *Senior Member, IEEE*,
Viet T. Vu, *Senior Member, IEEE*, Renato Machado, *Senior Member, IEEE*,
Bartolomeu F. Uchôa-Filho, *Senior Member, IEEE*, Patrik Dammert, *Senior Member, IEEE*,
and Hans Hellsten, *Senior Member, IEEE*

Abstract— This letter presents two new change detection (CD) methods for synthetic aperture radar (SAR) image stacks based on the Neyman–Pearson criterion. The first proposed method uses the data from wavelength–resolution images stack to obtain background statistics, which are used in a hypothesis test to detect changes in a surveillance image. The second method considers *a priori* information about the targets to obtain the target statistics, which are used together with the previously obtained background statistics, to perform a hypothesis test to detect changes in a surveillance image. A straightforward processing scheme is presented to test the proposed CD methods. To assess the performance of both proposed methods, we considered the coherent all radio band sensing (CARABAS)-II SAR images. In particular, to obtain the temporal background statistics required by the derived methods, we used stacks with six images. The experimental results show that the proposed techniques provide a competitive performance in terms of probability of detection and false alarm rate compared with other CD methods.

Index Terms— Coherent all radio band sensing (CARABAS) II, change detection (CD) methods, image stack, very-high-frequency (VHF) ultrawideband (UWB) synthetic aperture radar (SAR).

I. INTRODUCTION

WAVELENGTH–RESOLUTION very-high-frequency (VHF) airborne synthetic aperture radar (SAR) systems' design and their applications have been investigated for decades [1]. These systems are characterized by a large fractional bandwidth, e.g., ultrawideband (UWB), and a wide antenna bandwidth, resulting in resolutions cells in

the order of the radar signal wavelengths [2]. The main contributions for wavelength–resolution SAR systems come from large scatterers, with dimensions in the order of the signal wavelengths. Usually, there is at most one such a scatterer with significant contribution in a resolution cell, and as a result, the images do not effectively suffer from speckle noise [3], [4]. For systems operating at these frequency ranges, such as the coherent all radio band sensing (CARABAS) II [5], the main contributions come from large scatterers, e.g., tree trunks and human-made structures. These objects tend to be stable in time between different measurements [3].

One of the main applications considered to exploit the benefits provided by the wavelength–resolution VHF SAR data is change detection (CD) [5]– [10]. Most of the CD methods consider the use of one surveillance image and one reference image to apply in different statistical models for the clutter plus noise distribution. These models are generally used in hypothesis tests based on the Neyman–Pearson (NP) criterion [11]. For instance, the CD method proposed in [8] considers that the clutter plus noise can be modeled as a Gaussian distribution. However, it is important to highlight that the authors in [8] mention that using more accurate models could provide better performances. Studies considering different statistical models for the background were published using the Gamma distribution [10], Rayleigh, and K-distributions [12].

A recent research topic related to CD in wavelength–resolution images is the use of small image stacks in the processing schemes. Even knowing that the use of image stacks for traditional SAR system applications is a frequent topic [13], especially for polarimetric images [14], their use in CD methods for wavelength–resolution images was first introduced in [9], to the best of our knowledge. In [9] and [10], the authors show that the use of image stacks can provide an improvement in CD methods performance by reducing the occurrence of false alarms (FA). More recently, in [2], statistical analysis for wavelength–resolution SAR image stacks was proposed. That study provides some insights into the use of image stacks to assess their background statistics.

Motivated by the observation about the use of accurate clutter models in [8] and by the promising results in [9] and [10], in this letter, we present two new CD methods

for SAR wavelength–resolution image stacks, focusing on target detection applications. The first method only uses the background statistics to perform a hypothesis test based on NP, which is criterion-based only on the background statistics. The second method considers assumptions on target statistics to perform a hypothesis test based on the NP criterion.

To assess the performance of the proposed methods, we considered a dataset obtained by the CARABAS II SAR system. The results reveal that both proposed methods have competitive performance compared with other recently proposed methods. The main contributions of this letter are given as follows:

1) the use of wavelength–resolution SAR image stacks to obtain the background statistics based on the "stack domain," as described in [2], granting the possibility of using any number of SAR images into the methodology;

2) the proposition and evaluation of two new CD methods for wavelength–resolution image stacks using the background statistics obtained from the image stack.

Sections II–V are organized as follows. Section II presents the dataset used in this letter and the definition of the background statistics obtained from image stacks. Section III presents both proposed CD methods for wavelength–resolution SAR image stacks based on the NP criterion. Section IV presents some implementation aspects and the experimental evaluation of the proposed techniques. Finally, some concluding remarks are provided in Section V.

II. DATA DESCRIPTION

Both proposed methods are designed for VHF wavelength–resolution SAR images. This kind of image is characterized by their time stability, for not effectively suffering from the speckle noise, and their low sensibility to small scatterers [2], [3]. In this letter, we use the dataset available in [15] and presented in [5] and [8], which was obtained using the CARABAS II system. The CARABAS II system is a VHF UWB SAR with a spatial resolution in the order of 2.5 m in both azimuth and range dimensions. The dataset consists of 24 wavelength–resolution amplitude images that cover the ground area of 6 km² (3 km × 2 km) and are given in the form of a 3000 × 2000 matrix [5]. The given images are already calibrated, preprocessed, and geocoded.

The flight campaigns were held in the military base station Missile Test Area North (RFN) Vidsel in 2002. The testing site is composed mainly of forest areas but also lakes, human-made structures, and fields. The measurements contain 25 testing targets, which consist of terrain vehicles divided by their sizes. The targets consist of ten "small" size TGB11 vehicles, eight "medium" size TGB30 vehicles, and seven "large" size TGB40 vehicles [5].

The 24 images are divided considering four different target deployments (missions), which are measured using six distinct passes. The passes are classified according to their flight geometry and the intensity of radio frequency interference. More information regarding the CARABAS II dataset can be obtained in [5], [8], and [15]. The dataset is equally divided into three stacks composed of images with the same flight geometry. Accordingly, the images obtained with passes 1 and 3 form Stack 1, while Stack 2 is formed with
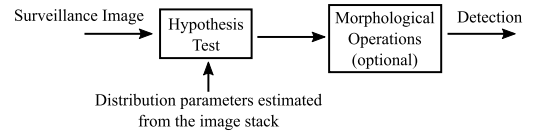

Fig. 1. Simplified diagram block for the proposed CD methods.

the images obtained with passes 2 and 4, and the others build Stack 3.

A. Background Statistics

The background statistics are obtained from the images of the same stack, in a temporal way, since they have similar scattering properties. The results presented in [2] show that the background statistics for SAR wavelength–resolution image stacks can be modeled as a Rician distribution. Based on the available CARABAS II dataset, each stack could have a maximum of eight images. However, to perform the CD method, the images with the same target deployment (mission) as the surveillance image should be excluded from the stack used to obtain the background statistics. Thus, the background distribution parameters are obtained from data of six images from the same stack, using a maximum likelihood estimator, over the domain of the distribution function, and using the methodology of pixel selection considered and discussed in [2], which consists of using a resolution cell sample per image resulting in a total of 6×9 pixels per estimation. Other methodologies may be used to obtain the background statistics, e.g., the downsampling and filtering processes, which could provide better performance.

III. PROPOSED CD METHODS

The proposed CD methods consist of statistical hypothesis tests based on the NP criterion and temporal background statistics obtained from the image stack, as described in Section II-A. A simplified block diagram for the processing of both CD methods is presented in Fig. 1. According to the processing scheme, the method inputs are one surveillance image and the parameters of the background distribution, i.e., the Rician distribution, which are obtained from the image stack and, if available, information from the target statistics. In this letter, we focus on target detection.

The first block is a hypothesis test applied in each pixel position from the image stack, resulting in a total of six million evaluations for this dataset. Both proposed CD methods are based on the NP criterion [11]. For a particular pixel position in the surveillance image, this criterion can be written as

$$\frac{p_{(i,j)}(x|H_1)}{p_{(i,j)}(x|H_0)} \underset{H_0}{\overset{H_1}{\gtrless}} \tau \qquad (1)$$

where τ is a threshold, H_0 is the hypothesis that the evaluated pixel is background-related, and H_1 is the hypothesis that the evaluated pixel is target-related (change). The hypothesis tests of the proposed CD methods are discussed in Sections III-A and III-B, respectively.

It is added one block of morphological operations, which is optional. The output of the processing scheme is a binary image that contains the detected targets and FA (if any). Finally, it is noticeable that the proposed methods only differ from each other in the hypothesis test block.
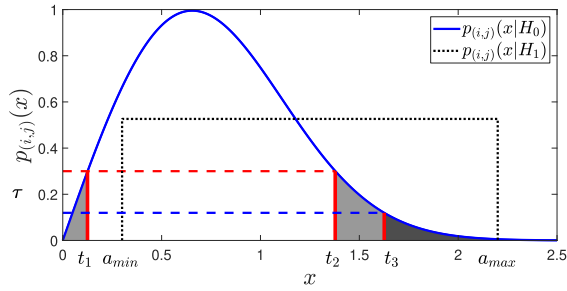
Fig. 2. Representation of the hypothesis tests (1) and (2) for a given sample of $p_{(i,j)}(x|H_0)$ modeled as a Rician distribution with $\sigma = 0.5$ and $\nu = 0.5$ and $p_{(i,j)}(x|H_1)$ modeled as a Uniform distribution. The gray highlighted areas are related to the FAs considering x-axis projections of the thresholds τ, represented by t_1, t_2, and t_3, which are represented by the red and blue dashed lines, respectively, for the first and second proposed methods.

Fig. 3. CDF for different values of $\nu_{i,j}$.

A. CD Method Based on NP Using Only Background Statistics (NPCBS)

Most of the practical applications using CD techniques do not have enough information on the target statistics. Generally, only the background distribution is characterized. A detection criterion can be used to avoid assumptions for the distribution $p_{(i,j)}(x|H_1)$, as the method presented in [16]. In this method, an image sample would be assigned as a target if

$$p_{(i,j)}(x|H_0) \leq \tau. \tag{2}$$

Examples of the hypothesis tests (1) and (2) are presented in Fig. 2. In general, CD applications focus on targets that are present in the tail of the distributions. Thus, the area over the interval $x < t_1$ can be disregarded. Besides, for most distributions considered for this kind of application, this area will present a small value compared with the area for $x > t_2$. Thus, the FA probability (P_{FA}) for a given sample using the detection criterion (2) can be written as

$$P_{FA} \approx \int_{t_2}^{\infty} p_{(i,j)}(x|H_0)dx. \tag{3}$$

Based on (3), it is possible to define t_2 for each sample given a fixed FA probability. Thus, it is possible to define the threshold $\tau = p_{(i,j)}(t_2|H_0)$. Substituting it into (2), we have that

$$p_{(i,j)}(x|H_0) \leq p_{(i,j)}(t_2|H_0) \tag{4}$$

which results in the detection criteria $x \geq t_2$. After some simple manipulations, it is possible to rewrite the detection criterion of (2) in terms of the background cumulative distribution function (CDF) and P_{FA}. The detection criterion can be written as

$$P_{B(i,j)}(x_{i,j}) \geq 1 - P_{FA} \tag{5}$$

where $P_{B(i,j)}(\cdot)$ is the background CDF.

The detection criterion (5) is used in the CD method based on NP using only background statistics (NPCBS). This criterion directly relates the background CDF for a given sample with a P_{FA} constant. For traditional SAR CD scenarios, background statistics are obtained from local regions generally characterized by several pixels from the desired sample window of the image; this criterion detects any sample
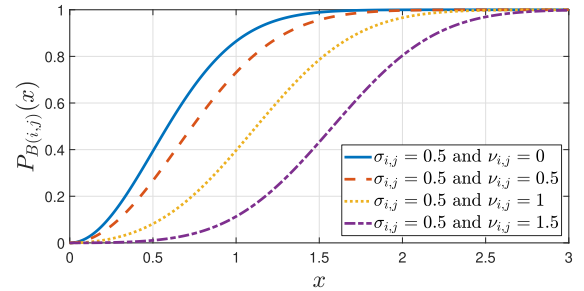
that contains a high amplitude as a target, which could result in a large number of FAs [16].

To overcome this problem, we consider the nontraditional methodology proposed in [2] to obtain the background statistics for a given pixel sample, considering image stacks. Thus, without loss of generality, the constant τ can be converted into a function of the pixel position $\tau(x)$, for a fixed P_{FA}. This procedure can be performed using (4) for each pixel position, considering its estimated parameters.

As observed in [2], the background statistics samples can be modeled as a Rician distribution, which is based on the parameters $\sigma_{i,j}$ and $\nu_{i,j}$. Thus, the background samples related to strong scatterers tend to present high values of $\nu_{i,j}$. Considering the Rician distribution, the higher is the value of $\nu_{i,j}$, the smoother is the inclination of the sample CDF, as can be observed in Fig. 3. Consequently, for a fixed P_{FA}, the higher is the $\nu_{i,j}$ parameter, the higher will be the x-axis projection of threshold. Thus, the detection criterion (5) applies different thresholds for the tested pixels to avoid most of the FAs related to the region with strong scatterers without targets. The proposed CD method consists of the processing scheme from Fig. 1, considering the hypothesis test (5) using the temporal background statistics from the image stack.

B. CD Method Based on NP-Criterion (NPC)

The detection criterion presented in (5) directly relates the background CDF with a fixed FA probability constant and only requires information about the background statistics. However, for some CD applications, there is some information available on the target statistics, which can be exploited to improve the method performance. Under these conditions, it is possible to consider the detection criterion (1).

For wavelength–resolution SAR images, we can assume that the targets tend to have an amplitude signature that ranges from a minimum amplitude a_{min} to a maximum amplitude a_{max}, as considered in [6] and [7]. Moreover, based on the aforementioned characteristics of this type of image, e.g., near speckle-free images, and considering a specific kind of targets, it is possible to assume that the distributions of the different targets tend to be similar. Following the methodology considered in [6] and [7], we assume that the targets follow a uniform distribution.

Based on the previous distributions assumptions, the CD method based on NP-criterion (NPC) consists of the processing scheme from Fig. 1, considering the hypothesis test presented in (1) using the background statistics obtained from

the image stack. Fig. 2 also presents one example of the hypothesis test (1) with the previously mentioned considered distributions, where t_3 is the x-axis projection of the threshold τ. Similar performance analysis in terms of the P_{FA} metric as the one done for the NPCBS method can also be done for the NPC method. P_{FA} for a given sample, considering $a_{\min} \leq t_3$ and $a_{\max} > t_3$, can be written as

$$P_{FA} = \int_{t_3}^{a_{\max}} p_{(i,j)}(x|H_0)dx \approx 1 - \int_0^{t_3} p_{(i,j)}(x|H_0)dx \quad (6)$$

where $a_{\min}$ and $a_{\max}$ should be selected according to the target-related assumptions, as will be discussed in Section IV-A. Note that, if $a_{\min} \geq t_3$, the integrand limits would be $[a_{\min}, a_{\max}]$. For instance, considering the assumption of a $a_{\min} \leq t_3$ and $a_{\max} \to \infty$, and after some simple manipulations, it is possible to obtain the scenario with maximum P_{FA}, which can be written as

$$1 - P_{FA} \approx P_{B(i,j)}(t_3). \quad (7)$$

Thus, in the worst case scenario, a similar P_{FA} is expected for both proposed methods. Moreover, a P_{FA} performance gain is expected for the NPC method under better selected values of $a_{\min}$ and $a_{\max}$. However, this performance gain may result in the impossibility of detecting some targets, e.g., the target amplitude is lower than $a_{\min}$, reducing its detection probability. Finally, from (7), t_3 can be written as

$$t_3 \approx Q(1 - P_{FA}) \quad (8)$$

where Q is the Quantile function and t_3 is related to the threshold $\tau = p(t_3|H_0)$, which would result in the same threshold as the one used in the NPCBS method. However, it is important to emphasize that, even using the same or similar detection thresholds, the detection criteria for NPCBS and NPC, represented, respectively, by (5) and (1), are different and tend to present different detection performances.

IV. EXPERIMENTAL RESULTS

The experimental evaluation of the proposed CD methods based on image stacks considers all the 24 images from the dataset presented in Section II, which is also used in [5], [10], and [17]. The methods' performance is assessed in terms of the probability of detection (P_d), i.e., the ratio of the number of detected targets to the known number of targets, and false alarm rate (FAR)—here defined as the number of FAs per square kilometer. For this analysis, every object detected by the methods was considered as a change, even knowing that some of them could be related to the radar system, e.g., antenna back lobe or image formation issues, such as radio frequency interference suppression.

A. Implementation Aspects

The parameters of the distribution $p_{(i,j)}(x|H_1)$, $a_{\min}$ and $a_{\max}$, are selected according to assumptions about the targets. For the studied dataset, it is expected that pixels related to the targets present higher amplitudes compared with clutter-related pixels. Moreover, there is no information regarding the maximum amplitude of target-related pixels. Thus, according the methodology employed in [10], we use the set of values

$a_{\min} \in [0.2; 0.3; 0.4]$. Besides, for the sake of simplicity, we adopted $a_{\max}$ as the highest pixel-amplitude value of the surveillance image. It is important to highlight that more information on the targets can be used to consider the use of a better-matched distribution $p_{(i,j)}(x|H_1)$ to improve the proposed method performance. The methodology described in Section III-B only guarantees that the performance of the NPC method will be equal or better than the NPCBS in terms of FA probability. A bad choice of the distribution $p_{(i,j)}(x|H_1)$ or its parameters can result in worse performances in terms of P_d or even the failure to detect targets for any threshold.

The threshold selection for the method NPCBS is based on (5), for different constant values of $P_{FA} = 10^{-n}$, where $n \in [1, 2, 3, \ldots]$. For the NPC CD method, the threshold can be obtained by using (6) and (4) considering t_3. However, this selection requires a large number of mathematical operations due to the necessity to calculate the quantile function for every tested pixel. Based on the number of tested images and their sizes, this selection becomes unpractical. To simplify the threshold selection, we considered for the experimental evaluations $\tau = 10^k$, where $k \in [0, 1, 2, 3, \ldots]$, which guarantees $p_{(i,j)}(x|H_1) \geq p_{(i,j)}(x|H_0)$ and overcomes computational complexity issue for this dataset. For situations with less tested pixels, the threshold selection considering the derivation presented in Section III-B becomes more suitable.

Finally, to perform a fair comparison between the evaluated methods, we use similar morphological operations to the ones considered in [8], [10], and [17]. The morphological operations used herein are one erosion followed by two dilatations. The erosion considers the system resolution cell size, and it is used to remove isolated pixels detected as changes. The dilatations consider sizes that enable merging any detected samples that are separated by up to ten meters.

B. Methods Evaluation

Initially, we compare the performance of the proposed methods with the performance of previous methods published in the literature in terms of the receiver operating characteristic (ROC) curves. First, we present one analysis to validate the use of image stacks in CD methods. This analysis consists of a comparison between the proposed methods based on image stacks and others based on the use of only one reference image. For this analysis, two methods were selected. The first method is presented in [8], which was one of the first techniques used to perform CD in CARABAS II data. The other one is the method proposed in [10], which has, to the best of our knowledge, the best performance for the CARABAS II data, without considering an image stack scenario. This comparison is presented in Fig. 4. For the comparison, only the two best ROC curves presented in [10] and the best ROC curve presented in [8] are shown in Fig. 4. Finally, the original notations presented in [8] and [10] were kept for simplicity.

As can be observed in Fig. 4, the proposed methods outperform the other evaluated ones in terms of probability of detection and FAR, excluding the saturation region for $a_{\min} = 0.4$. These results corroborate the use of image stacks to improve the performance of CD methods in terms of probability of detection and FAR. Based on the similar target amplitude considerations, it is observable that both
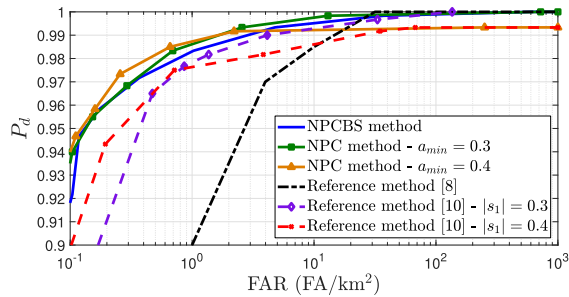
Fig. 4. ROC performance for the proposed and reference methods. The reference ROC curves are the best one presented in [8] and the two best results presented in [10].
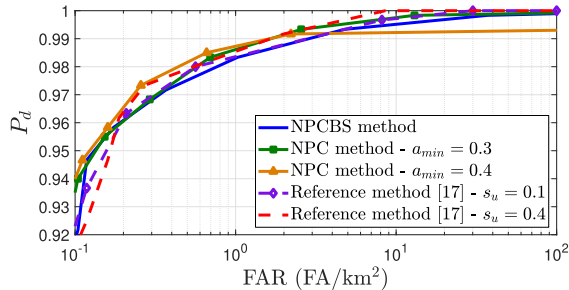

Fig. 5. ROC performance for the proposed and reference methods. The reference curves are the two best results presented in [17].

methods present a saturation in the probability of detection for $a_{\min} = |s_1| = 0.4$.

We present a comparison between the proposed methods and the technique in [17], which are based on image stacks. To the best of our knowledge, the method presented in [17] had the best performance in terms of P_d and FAR so far. This method considers the subtraction of two reference images with the same target deployment to be used in the hypothesis test associated with a surveillance image. This comparison is presented in Fig. 5, considering only the best ROC curves presented in [17].

As can be observed in Fig. 5, the proposed methods have similar performance compared with the method of [17]. It is possible to state that the NPC method with $a_{\min} = 0.4$ and the NPCBS present better performance than the best ROC curve of the reference method for $P_d \leq 0.99$ and $P_d \leq 0.959$, respectively. Moreover, the proposals presented in this letter enable the use of more images in the stack, providing better estimations of $p_{(i,j)}(x|H_0)$. As a result, different methodologies could be used to obtain the background statistics compared to the one presented in Section II-A. A brief discussion about this issue is considered in [2]. The methods do not require that the reference images contain the same target deployment. In fact, these characteristics enable the use of the proposed method in more applications. Finally, it is important to state that the NPC performance can be further improved when more *a priori* information about the targets is available.

V. CONCLUSION

This letter presented two new CD methods for wavelength–resolution SAR image stacks based on the NP criterion. The two proposed methods are better suited for the following two scenarios, with and without information

on the target's statistics. The proposed methods were both evaluated in terms of detection probability and FAR considering a dataset of 24 incoherent images obtained with the CARABAS II system. The hypothesis tests used six SAR images in their methodology to obtain the required temporal background statistics. The experimental results show that the use of image stack provides better performance than methods that do not consider the use of image stacks, in terms of both evaluated metrics. Besides, both proposed methods presented a competitive performance compared with other existing image stack-based methods. Based on the previous results, it is possible to state that the proposed methods have one of the best performances, up until now, for the tested dataset. Finally, the proposed methods have fewer application constraints than the other ones based on image stacks, which have already been tested with the CARABAS II dataset.

REFERENCES

[1] H. Hellsten *et al.*, "Ultrawideband VHF SAR design and measurements," *Proc. SPIE*, vol. 2217, pp. 16–25, Jul. 1994.

[2] D. I. Alves *et al.*, "A statistical analysis for wavelength-resolution SAR image stacks," *IEEE Geosci. Remote Sens. Lett.*, vol. 17, no. 2, pp. 227–231, Feb. 2020.

[3] R. Machado, V. T. Vu, M. I. Pettersson, P. Dammert, and H. Hellsten, "The stability of UWB low-frequency SAR images," *IEEE Geosci. Remote Sens. Lett.*, vol. 13, no. 8, pp. 1114–1118, Aug. 2016.

[4] G. Smith and L. M. H. Ulander, "A model relating VHF-band backscatter to stem volume of coniferous boreal forest," *IEEE Trans. Geosci. Remote Sens.*, vol. 38, no. 2, pp. 728–740, Mar. 2000.

[5] M. Lundberg, L. M. H. Ulander, W. E. Pierson, and A. Gustavsson, "A challenge problem for detection of targets in foliage," *Proc. SPIE*, vol. 6237, May 2006, Art. no. 62370K.

[6] H. Hellsten, R. Machado, M. I. Pettersson, V. T. Vu, and P. Dammert, "Experimental results on change detection based on bayes probability theorem," in *Proc. IEEE Int. Geosci. Remote Sens. Symp. (IGARSS)*, Jul. 2015, pp. 318–321.

[7] H. Hellsten and R. Machado, "Bayesian change analysis for finding vehicle size targets in VHF foliage penetration SAR data," in *Proc. IEEE Radar Conf.*, Oct. 2015, pp. 510–515.

[8] L. M. H. Ulander, M. Lundberg, W. Pierson, and A. Gustavsson, "Change detection for low-frequency SAR ground surveillance," *IEE Proc.-Radar, Sonar Navigat.*, vol. 152, no. 6, pp. 413–420, Dec. 2005.

[9] V. T. Vu, M. I. Pettersson, R. Machado, P. Dammert, and H. Hellsten, "False alarm reduction in wavelength-resolution SAR change detection using adaptive noise canceler," *IEEE Trans. Geosci. Remote Sens.*, vol. 55, no. 1, pp. 591–599, Jan. 2017.

[10] V. T. Vu, N. R. Gomes, M. I. Pettersson, P. Dammert, and H. Hellsten, "Bivariate gamma distribution for wavelength-resolution SAR change detection," *IEEE Trans. Geosci. Remote Sens.*, vol. 57, no. 1, pp. 473–481, Jan. 2019.

[11] J. Neyman and E. S. Pearson, "On the problem of the most efficient tests of statistical hypotheses," *Phil. Trans. Roy. Soc. London. Ser. Containing Papers Math. Phys. Character*, vol. 231, nos. 694–706, pp. 289–337, 1933.

[12] N. R. Gomes, P. Dammert, M. I. Pettersson, V. T. Vu, and H. Hellsten, "Comparison of the Rayleigh and K-Distributions for application in incoherent change detection," *IEEE Geosci. Remote Sens. Lett.*, vol. 16, no. 5, pp. 756–760, May 2019.

[13] M. J. Sanjuan-Ferrer, I. Hajnsek, K. P. Papathanassiou, and A. Moreira, "A new detection algorithm for coherent scatterers in SAR data," *IEEE Trans. Geosci. Remote Sens.*, vol. 53, no. 11, pp. 6293–6307, Nov. 2015.

[14] D. Ciuonzo, V. Carotenuto, and A. De Maio, "On multiple covariance equality testing with application to SAR change detection," *IEEE Trans. Signal Process.*, vol. 65, no. 19, pp. 5078–5091, Oct. 2017.

[15] U.S. Air Force. *The Sensor Data Management System-SDMS*. Accessed: Mar. 26, 2018. [Online]. Available: https://www.sdms.afrl.af.mil/

[16] C. Oliver and S. Quegan, *Understanding Synthetic Aperture Radar Images*, 1st ed. Boston, MA, USA: SciTech, 2004.

[17] V. T. Vu, "Wavelength-resolution SAR incoherent change detection based on image stack," *IEEE Geosci. Remote Sens. Lett.*, vol. 14, no. 7, pp. 1012–1016, Jul. 2017.